Linking microscopic and macroscopic response in disordered solids

Daniel Hexner, Andrea J. Liu, and Sidney R. Nagel

Linking microscopic and macroscopic response in disordered solids

Daniel Hexner*

The James Franck Institute and Department of Physics, The University of Chicago,
Chicago, IL 60637, USA and Department of Physics and Astronomy,
The University of Pennsylvania, Philadelphia, PA, 19104, USA

Andrea J. Liu

Department of Physics and Astronomy, The University of Pennsylvania, Philadelphia, PA, 19104, USA

Sidney R. Nagel

The James Franck and Enrico Fermi Institutes and The Department of Physics,
The University of Chicago, Chicago, IL 60637, USA

The modulus of a rigid network of harmonic springs depends on the sum of the energies in each of the bonds due to an applied distortion such as compression in the case of the bulk modulus or shear in the case of the shear modulus. However, the distortion need not be global. Here we introduce a *local* modulus, L_i, associated with changing the equilibrium length of a single bond, i, in the network. We show that L_i is useful for understanding many aspects of the mechanical response of the entire system. It allows an efficient computation of how the removal of any bond changes the global properties such as the bulk and shear moduli. Furthermore, it allows a prediction of the distribution of these changes and clarifies why the changes of these two moduli due to removal of a bond are uncorrelated; these are the essential ingredients necessary for the efficient manipulation of network properties by bond removal.

I. INTRODUCTION

Disordered spring networks are a common starting point for studying the mechanical properties of amorphous materials. On the microscopic level, the stress distribution due to any deformation forms complicated non-affine patterns strongly depending on details of the network structure. At large length scales, this microscopic complexity becomes irrelevant for small deformations. The response to such deformations is well described by continuum elasticity[1] in terms of a small number of elastic constants. When the system is isotropic there are only two relevant elastic constants, the bulk modulus, B, and a single shear modulus, G.

Inevitably in a disordered system, some regions must be softer than others. In glasses, such regions can preferentially fail under strain via particle rearrangements [1–4]. Similarly, when disordered networks are placed under strain, bonds under large stresses are more likely to fail than those under smaller stress [5, 6]. When bonds break, the global moduli decrease by amounts that depend on the details of the broken bonds. This bond-to-bond variation can be exploited to manipulate the elastic properties of a solid by removing select bonds [7]. Indeed, it has been shown that disordered networks are highly tunable so that the ratio of the shear to bulk modulus, G/B, can be varied over nearly twenty orders orders of magnitude by removing only of order 1% of the bonds [7]. This allows the design of auxetic metamaterials.

In this paper we explore the relation between microscopic local bond properties and macroscopic elastic moduli. Our key insight is that an important quantity in understanding this link is a new "local modulus", L_i, which measures the modulus associated with pinching a bond. This modulus is a measure of the local rigidity that characterizes the propensity of a bond to carry stress under a global deformation. Using the local modulus, we derive an exact linear-response relation that predicts how an arbitrary modulus, M, will change when bond i is removed. In this paper, we are primarily interested in the cases where M represents either the bulk or the shear modulus.

We find that ΔM_i, the change in modulus M when bond i is removed, depends on both the local modulus, L_i, and the stress in bond i due to the applied deformation. By analyzing the relationship of L_i to the global moduli we show that there are only weak correlations between ΔB_i and ΔG_i. Our theoretical arguments, supported by numerical simulations, also indicate that the distribution of ΔG_i, and in many cases also ΔB_i, obeys a universal functional form. In addition, we demonstrate that the distribution of L_i is governed by the critical properties of packings from which the networks are derived. This analysis gives insight into the local elasticity of disordered networks and is useful in the design of meta-materials.

II. DERIVATION OF THE RELATION: $\Delta M_i = k_i M_i / L_i$

We will consider the simplest model of a mechanical network, in which nodes are connected by unstretched central-force harmonic springs. The total energy due to a

deformation is the sum of the energy on all the individual springs, labeled by i:

$$E = \frac{1}{2}\sum_i k_i \left(\delta x_i\right)^2 = \frac{1}{2}\sum_i t_i^2/k_i \qquad (1)$$

where k_i are the spring constants, δx_i are the spring extensions and t_i are the stresses on the bonds. Both the δx_i and the t_i depend on the deformation applied to the system and will be different for compression and shear.

The additive nature of the energy allows us to decompose any modulus M into the sum of individual bond contributions: $M = \sum_i M_i$ [7], where $M_i = 2k_i\left(\delta x_i\right)^2/V$, where V is the volume. Our aim is to calculate ΔM_i, the change in M due to the removal of bond i.

We consider an infinitesimal perturbation that alters the equilibrium length of the single spring, i, by an amount $\delta\ell_i$. This local strain perturbation leads to stresses on all the springs. The total energy, E^i, is the sum of all the bond energies: $E^i = \frac{1}{2}\sum_j (t_j^i)^2/k_j$. (The superscript on E^i and t^i represents the applied deformation – in this case the perturbation in the length of spring i.) We define the local modulus $L_i \equiv 2E^i/\delta\ell_i^2$. We note that L_i is "local" only in the sense that the applied deformation is restricted to a single bond. The resulting stresses typically decay as a power-law function of distance [8] and are not local. We also emphasize that L_i is distinct from previous definitions of local moduli that are defined as the response of a finite region of the system [9].

For simplicity, we consider all springs to have the same spring constant, k. (Appendix A Information shows that this exact relation is also true in the general case where k_i can be different on each bond.) The derivation is based on the formalism of states-of-self-stress [10, 11], which are the set of combinations of tensions $\{t_i\}$ resulting in force balance on all nodes . In the following we use the bra-ket notation, where $|v\rangle$ denotes a vector, $\langle v|$ its transpose, v_i its ith component and the inner product $\langle v\mid u\rangle = \sum_i v_i u_i$. We use α and β to index these states of self stress: $s_{\alpha,i}$ is the tension on bond i in the state $|s_\alpha\rangle$. Typically, there are an extensive number of such combinations and we define an orthonormal basis satisfying $\langle s_\alpha\mid s_\beta\rangle = \delta_{\alpha,\beta}$.

Within linear response the energy of a deformation, derived in [12–15], can be expressed in terms of $|s_\alpha\rangle$ and $\left|e^M\right\rangle$, the bond extensions resulting from the affine contribution to the deformation giving rise to the modulus M (For example, this would be compression in the case of the bulk modulus.). The idea behind this calculation involves performing the deformation in two stages. First, the system is deformed in an affine manner (hence the dependence on e_i^M). When there is disorder, the affine deformation does not satisfy force balance; as a result there will be forces on the nodes and stresses on the bonds. Subsequently, the system is allowed to relax to the final mechanical equilibrium. The stresses that cannot be eliminated by the motion of the nodes are those that satisfy force balance, spanned by the states of self stress. The resulting energy and bond tensions are:

$$E^M = \frac{k}{2}\sum_{\alpha=1}^{N_s}\left\langle s_\alpha\mid e^M\right\rangle^2, \qquad (2)$$

$$\left|t^M\right\rangle = k\sum_{\alpha=1}^{N_s}\left\langle s_\alpha\mid e^M\right\rangle|s_\alpha\rangle, \qquad (3)$$

where N_s is the number of states of self stress. The systems we consider are rigid, implying that $N_s \geq d(d+1)/2$ which correspond to the number of independent global deformations [14]. The affine bond extensions are denoted by $e_i^M = \sum_{\mu\nu}\delta r_{i,\mu}\epsilon_{\mu\nu}^M\delta\hat{r}_{i,\nu}$ and depend on the strain tensor $\epsilon_{\mu\nu}^M$ corresponding to the applied deformation and the bond vector δr_i. Here μ and ν index the spatial coordinates.

There is large degeneracy in choosing a basis since any linear combination of $|s_\alpha\rangle$ is also a state of self stress. For convenience we choose $|s_1\rangle$ to be in the direction of $\left|e^M\right\rangle$ so that $\left\langle e^M\mid s_{\alpha\neq1}\right\rangle = 0$ and only the $\alpha = 1$ term contributes to the deformation energy [16]. With this choice of basis,

$$M_i = Ms_{1,i}^2. \qquad (4)$$

where the modulus $M = \frac{k}{V}\left\langle e^M\mid s_1\right\rangle^2$ and V is the volume.

In order to compute ΔM_i, the change in a modulus after bond i is removed, we need a new basis in the pruned network, $|s'_\alpha\rangle$. Fortunately, this can be expressed using $|s_\alpha\rangle$ of the unpruned network. To see this, we note that any linear combination of $|s_\alpha\rangle$ which has zero tension on bond i is also a state of self stress of the pruned network, since force balance is still obeyed.

We introduce a new state of self stress that depends on i, the targeted bond: $|S_i\rangle = \sum_{\alpha=1}^{N_s}s_{\alpha,i}|s_\alpha\rangle$. $|S_i\rangle$ is independent of the choice of basis and has several nice properties. First, using Eq. 3 with $e_j^i = \delta_{ij}$, one can verify that the stress on bond j resulting from a unit change in equilibrium length of bond i is $t_j^i = kS_{i,j} = kS_{j,i}$[17]. We can compute the energy from these values of the stresses, $E^i = \frac{1}{2}k\sum_j S_{i,j}^2$. We also compute the energy from Eq. 2 using $e_j^i = \delta_{ij}$ [18]:

$$E^i = \frac{k}{2}\sum_{\alpha=1}^{N_s}s_{\alpha,i}^2 = \frac{k}{2}S_{i,i}. \qquad (5)$$

This implies that $L_i = kS_{i,i} = kS_i^2 \equiv k\langle S_i\mid S_i\rangle$ is the local modulus. Eq. 5 along with linear response formalism are used to compute S_i^2 numerically.

Using S_i^2 we now prove that, with our basis choice, the only state of self stress that contributes to the modulus M after bond i is removed is:

$$|s_1'\rangle = C\left(|s_1\rangle - \frac{s_{1,i}}{S_i^2}|S_i\rangle\right), \qquad (6)$$

and as a result stresses in the system are proportional to $|s_1'\rangle$ (here, $C = \left(1 - s_{1,i}^2/S_i^2\right)^{-1/2}$ is a normalization constant). To this end it must be shown that the remaining, $|s_{\alpha>1}'\rangle$, orthogonal to $|s_1'\rangle$, are orthogonal to the applied strain, $|e^M\rangle$. The vector space orthogonal to $|s_1'\rangle$ can be constructed explicitly from the $N_s - 1$ states of self stress $|s_{\alpha>1}\rangle$ using linear combinations of $|\tilde{s}_\alpha\rangle = s_{\gamma,i}|s_\alpha\rangle - s_{\alpha,i}|s_\gamma\rangle$, where both $\alpha > 1$ and $\gamma > 1$. This construction insures that the tension on the targeted bond i is zero. To see that these are orthogonal to $|s_1'\rangle$, we note that by the definition $\langle s_1 \mid \tilde{s}_\alpha\rangle = 0$, and that $\langle S_i \mid \tilde{s}_\alpha\rangle = 0$ as can be verified using the definition of $|S_i\rangle$. Since the basis vectors $|s_{\alpha>1}'\rangle$ are all linear combinations of $|s_{\alpha>1}\rangle$, which were chosen to be orthogonal to $|e^M\rangle$, also $\langle s_\alpha' \mid e^M\rangle = 0$ thus completing the proof.

Using Eq. 2 and noting that within linear response the modulus is proportional to elastic energy, the modulus after bond i is removed is therefore: $M' = \frac{k}{V}\left\langle e^M \mid s_1'\right\rangle^2$. The change in modulus, $\Delta M \equiv M - M'$ due to the removal of bond i, is $\Delta M_i = M_i/S_i^2$. As Appendix A shows, this result is valid for the more general case where the spring constants, k_i are not all equal:

$$\Delta M_i = M_i/S_i^2 = k_i M_i/L_i. \qquad (7)$$

This is the central equation on which our subsequent analysis is based.

III. NETWORKS CREATED FROM JAMMED CONFIGURATIONS

Our numerical results are based on networks derived from jammed packings of particles – a ubiquitous model for amorphous materials [19]. Configurations are prepared by standard methods[20, 21]; soft frictionless repulsive spheres are distributed randomly in space and the system's energy is minimized to produce a jammed configuration in which the coordination number, Z, exceeds the minimum required for stability, Z_{iso} [22].

The system is then converted into a spring network by replacing the spheres with springs connecting the centers of interacting particles. We remove any stresses by setting the equilibrium spring length to the inter-particle distance. Such networks capture many of the key properties of jammed packings [23], such as the scalings of the bulk and shear moduli [24]. We characterize these networks by their excess coordination, $\Delta Z \equiv (Z - Z_{iso})$. Since networks derived from packings do not have any zero modes (except for the trivial global translations and

rotations), the Maxwell-Caladine counting theorem predicts that at a constant ΔZ there are an extensive number of states of self stress, $N_s = N\Delta Z/2$. In this paper we focus on the case where $N_s \gg 1$.

IV. RELATION OF M_i TO S_i^2

In d-dimensions, there are $d(d + 1)/2 - 1$ independent shear moduli $\mathcal{G}$, which, if the system is isotropic, all have the same value, G. In this paper, we focus on two different global moduli M: the compression modulus B and the shear modulus corresponding to simple shear in the xy-direction, $\mathcal{G}^{ss} \equiv C_{xyxy}$. Our results hold as well for the other shear elastic constants, such as pure shear $\mathcal{G}^{ps} \equiv \frac{1}{4}\left(C_{xxxx} + C_{yyyy} - 2C_{xxyy}\right)$.

Equation 7, together with the condition that the generalized modulus is non-negative after bond removal, implies $M_i/M < S_i^2$. Both B_i and $\mathcal{G}_i^{ss}$ are strongly correlated with S_i^2. Figures 1a and 1b plot the conditional average of B_i and $\mathcal{G}_i^{ss}$ for a given value of S_i^2, denoted as $\langle B_i\left(S_i^2\right)\rangle$ and $\langle \mathcal{G}_i^{ss}\left(S_i^2\right)\rangle$. Excluding the largest values of S_i^2, both $\langle B_i\left(S_i^2\right)\rangle$ and $\langle \mathcal{G}_i^{ss}\left(S_i^2\right)\rangle$ are proportional to S_i^2. A plateau in $\langle B_i\left(S_i^2\right)\rangle$ exists at large S_i^2 that is more prominent in $d = 2$ (see Appendix B) The insets to Fig. 1a and 1b show that both $\langle \Delta B_i\left(S_i^2\right)\rangle$ and $\langle \Delta \mathcal{G}_i^{ss}\left(S_i^2\right)\rangle$ are nearly completely uncorrelated with S_i^2.

Varying ΔZ does not change $\langle \mathcal{G}_i^{ss}\left(S_i^2\right)\rangle$, but does change the overall magnitude of $\langle B_i\left(S_i^2\right)\rangle$, which scales as $\Delta Z^{-\lambda}$. In $d = 2$, $\lambda_{2D} \approx 1.4$ while in $d = 3$, $\lambda_{3D} \approx 1.0$. The average values of the modulus can be related to the conditional average. In $d = 3$:

$$\langle B_i\rangle = \int dS_i \langle B_i\left(S_i^2\right)\rangle P\left(S_i^2\right) \propto \Delta Z^{-\lambda_{3D}}\langle S_i^2\rangle, \quad (8)$$

$$\langle \mathcal{G}_i^{ss}\rangle = \int dS_i \langle \mathcal{G}_i^{ss}\left(S_i^2\right)\rangle P\left(S_i^2\right) \propto \langle S_i^2\rangle \qquad (9)$$

(where we substituted in the linear dependence of $\langle B_i\left(S_i^2\right)\rangle$ and $\langle \mathcal{G}_i^{ss}\left(S_i^2\right)\rangle$). Since as $\Delta Z \to 0$, $\langle B_i\rangle \to const$ and $\langle \mathcal{G}_i^{ss}\rangle \propto \Delta Z$, then $\langle S_i^2\rangle \propto \Delta Z^{\lambda_{3D}} \propto \Delta Z$, as also argued in Ref. [15] for any dimension. Therefore $\lambda_{3D} \approx 1$. This analysis fails in $d = 2$ for the bulk modulus because of the plateau at high S_i^2 in $\langle B_i\left(S_i^2\right)\rangle$.

The relation $\langle \mathcal{G}_i^{ss}\left(S_i^2\right)\rangle \propto S_i^2$ can be understood as follows. Note that $\mathcal{G}_i^{ss} = \frac{1}{2Vk}\left(t_i^{\mathcal{G}^{ss}}\right)^2$, where $t_i^{\mathcal{G}^{ss}}$ is the tension in a bond for a simple-shear deformation and V is the volume. Using Eq. 2: $t_i^{\mathcal{G}^{ss}} = k\sum_j e_j^{\mathcal{G}^{ss}}S_{i,j}$. For a simple-shear deformation $e_i^{\mathcal{G}^{ss}} = \frac{2}{|\delta r_i|}\delta r_{i,x}\delta r_{i,y} = \epsilon|\delta r_i|\sin(2\theta_i)$ where ϵ is the magnitude of the deformation, $|\delta r_i|$ is the length of the bond and θ_i is the bond angle with respect to the y-axis. If θ_i have only delta-function spatial correlations then $e_i^{\mathcal{G}^{ss}}$ can be considered uncorrelated random variables, with zero mean due to isotropy.
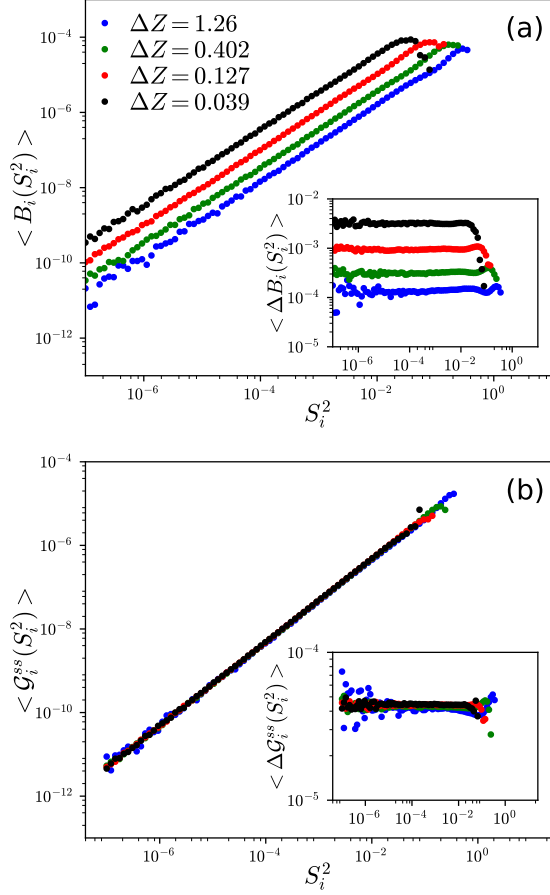
Figure 1. a) The conditional average $\langle B_i \left(S_i^2 \right) \rangle$ and b) $\langle \mathcal{G}_i \left(S_i^2 \right) \rangle$ are proportional to S_i^2 over a broad range of S_i^2. In the inset the corresponding $\langle \Delta B_i \left(S_i^2 \right) \rangle$ and $\langle \Delta \mathcal{G}_i \left(S_i^2 \right) \rangle$ are shown and to good approximation are independent of S_i^2. Data from 3d system with $N = 4096$ particles. See Appendix B for the 2d figure.

The inset to Fig. 2(b) shows that this is a good assumption. Lastly, we assume $S_{i,j}$ is not coupled to the value of a single $e_i^{\mathcal{G}^{ss}}$, and depends on the overall structure of the system so that the average is computed only over $e_i^{\mathcal{G}^{ss}}$ and $S_{i,j}$ is considered constant. Hence, $\langle \mathcal{G}_i^{ss} \left(S_i^2 \right) \rangle = \frac{1}{2Vk} \left\langle (e_i^{\mathcal{G}^{ss}})^2 \right\rangle \sum_j S_{i,j}^2$, leading to

$$\langle \mathcal{G}_i^{ss} \left(S_i^2 \right) \rangle \approx \frac{k}{2V} \left\langle (e_i^{\mathcal{G}^{ss}})^2 \right\rangle S_i^2. \qquad (10)$$

This approximation not only captures the dependence on S_i^2 but also predicts no additional dependence on ΔZ as found for ΔB_i. The derivation of Eq. 10 was based on the properties of $S_{i,j}$, the short-ranged bond angle correlations and isotropy. As a result, we expect this relation to hold quite generally for disordered networks.
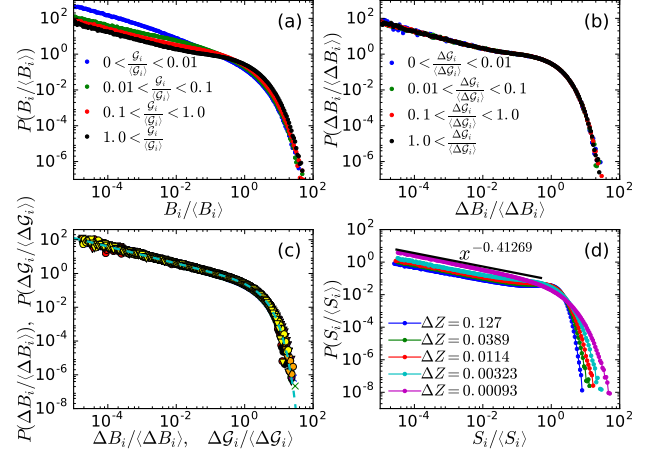

Figure 2. a) $P \left(B_i \right)$ for different ranges of $\mathcal{G}_i^{ss}$ and b) $P \left(\Delta B_i \right)$ for different range of $\Delta \mathcal{G}_i^{ss}$ at $\Delta Z = 0.127$. The collapse indicates almost vanishing correlations. c) The universal distribution of $P \left(\Delta \mathcal{G}_i^{ss} \right)$ for the pruned and unpruned case and the distribution of $P \left(\Delta B_i \right)$ for the pruned case. The cyan dashed line is the theoretical prediction $P \left(y \right) = \frac{1}{\sqrt{2\pi}} y^{-\frac{1}{2}} e^{-\frac{y}{2}}$. The distribution of $P \left(\Delta \mathcal{G}_i^{ss} \right)$ in the unpruned jammed network $\times$ blue $2d$, $\times$ green $3d$. The following pruning protocols lead to the same distribution where $P \left(\Delta B_i \right)$ is denoted by $\bullet$ and $P \left(\Delta \mathcal{G}_i^{ss} \right)$ is denoted by $\blacktriangledown$. The the number of removed bonds and dimensionality is also stated: red $max\Delta B_i$, $2d$, 50, black $max\Delta B_i$, $3D$ 30, purple $random$, 40, $2d$, orange $min\Delta \mathcal{G}_i^{ss}$, 40, $2d$ and yellow $max\Delta \mathcal{G}_i^{ss}$, 60 $2d$. d) $P \left(S_i^2 \right)$ for different values of ΔZ. Data from 3d system with $N = 4096$ particles. See Appendix B for the 2D figure.

V. CORRELATIONS BETWEEN B_i AND $\mathcal{G}_i$

In Ref. [7] it was argued that precise control over the ratio $\mathcal{G}^{ss}/B$ required independence of bond-level response. We have already shown in Fig. 1 that $\mathcal{G}_i^{ss}$ and B_i are both strongly correlated with S_i^2 and are therefore correlated with each other. However, our analysis shows that precise control over $\mathcal{G}^{ss}/B$ depends not on B_i and $\mathcal{G}_i^{ss}$, but on $\Delta B_i = B_i/S_i^2$ and $\Delta \mathcal{G}_i^{ss} = \mathcal{G}_i^{ss}/S_i^2$. Indeed, we find that the values of ΔB_i and $\Delta \mathcal{G}_i^{ss}$ are virtually uncorrelated with one another. We demonstrate this in Figs. 3(a) and (b). Fig. 3(a) shows that $P \left(B_i \right)$ depends on the range of $\mathcal{G}_i^{ss}$ being considered, in agreement with Ref. [7]. By contrast, the distribution, $P \left(\Delta B_i \right)$, is independent of the range of $\Delta \mathcal{G}_i^{ss}$, within numerical uncertainty. This implies very small correlations between ΔB_i and $\Delta \mathcal{G}_i^{ss}$.

In order to quantify the correlation between B_i and $\mathcal{G}_i^{ss}$, Ref. [7] used the Pearson correlation function, $r = \frac{\langle B_i \mathcal{G}_i^{ss} \rangle - \langle B_i \rangle \langle \mathcal{G}_i^{ss} \rangle}{\sigma_{B_i} \sigma_{\mathcal{G}_i^{ss}}}$ (where σ denotes the standard deviation and $\langle ... \rangle$ denotes the average) and found $r \approx 0.171$ in $d = 2$ and $r \approx 0.325$ in $d = 3$. In comparison, we find that for ΔB_i and $\Delta \mathcal{G}_i^{ss}$, the corresponding Pearson correlation

is $r < 0.05$ in $d = 2$ and $r < 0.01$ in $d = 3$. There is much less correlation than for B_i and $\mathcal{G}_i^{ss}$ [25]. The significant correlation between $\mathcal{G}_i^{ss}$ and B_i exists because both quantities are correlated with S_i^2.

Unlike perfect lattices, jammed systems are heterogeneous such that different bonds contribute differently to rigidity as characterized by S_i^2. This produces correlations between shear and compression since rigid regions, with a large average S_i^2, typically carry more stresses regardless of the type of deformation. Our results suggest that the correlation between B_i and $\mathcal{G}_i^{ss}$ can be estimated by assuming that $B_i = b_i \Delta Z^{-\lambda} S_i^2$ and $\mathcal{G}_i^{ss} = g_i S_i^2$, where b_i and g_i are uncorrelated random variables. This assumption leads to $\langle B_i \mathcal{G}_i^{ss} \rangle - \langle B_i \rangle \langle \mathcal{G}_i^{ss} \rangle \propto \Delta Z^{-\lambda} \left[\left\langle \left(S_i^2\right)^2 \right\rangle - \left\langle S_i^2 \right\rangle^2 \right]$ and gives the correct order of magnitude. There is also an additional small ΔZ dependence, such that the ratio of the left- and right-hand side varies by a factor of two over two orders of magnitude change in ΔZ. Presumably, this results from the plateau in $B_i \left(S_i^2\right)$ at large S_i^2 in Fig. 1.

VI. DISTRIBUTIONS FOR ΔM_i AND S_i^2

The distribution $P(B_i)$, shown in Fig. 2(a), is also shown along with $P(\mathcal{G}_i^{ss})$ in Fig. 1 of Ref. [7]. The distribution $P\left(\Delta B_i\right)$ is shown in Fig. 2(b), and $P\left(\Delta \mathcal{G}_i^{ss}\right)$ is shown in Fig. 2(c). Compared to $P(B_i)$ and $P(\mathcal{G}_i^{ss})$, $P\left(\Delta B_i\right)$ and $P\left(\Delta \mathcal{G}_i^{ss}\right)$ have a more robust power-law scaling at small values: $P\left(\Delta M_i\right) \propto \left(\Delta M_i\right)^{-\kappa}$ with a common value of the exponent: $\kappa \sim 0.5 \pm 0.03$. At large values the distributions decrease with roughly exponential tails. The most significant difference between $P\left(\Delta B_i\right)$ and $P\left(\Delta \mathcal{G}_i^{ss}\right)$ is evident at large values, where $P\left(\Delta B_i\right)$ develops a peak at large pressure while $P\left(\Delta \mathcal{G}_i^{ss}\right)$ continues to decay monotonically. The distributions of $P\left(\Delta \mathcal{G}_i^{ss}\right)$ are the same in $d = 2$ and $d = 3$.

Note that as bonds are pruned, the distributions $P\left(\Delta B_i\right)$ and $P\left(\Delta \mathcal{G}_i^{ss}\right)$ can evolve. We have therefore studied the robustness of these distributions to the removal of a small percentage of the bonds according to a variety of protocols. We can prune bonds at random or we can prune according to the maximum or minimum value of ΔM_i. In all cases there is little change in the functional form of the distribution $P\left(\Delta \mathcal{G}_i^{ss}\right)$. Remarkably, however, $P\left(\Delta B_i\right)$, which initially differs from $P\left(\Delta \mathcal{G}_i^{ss}\right)$, evolves to the same distribution as $P\left(\Delta \mathcal{G}_i^{ss}\right)$ in all but the case where we took away bonds with the smallest values of ΔB_i. We only need to remove approximately 0.5% of the bonds to achieve the collapse shown in Fig. 2(c). To a good approximation, this distribution is given by $P\left(\Delta M\right) = \frac{1}{\sqrt{2\pi}} y^{-0.5} e^{-\frac{y}{2}}$ (see Fig. 2(c)).

To understand this universal distribution, we note that the bond angles have only short-ranged correlations, the system is isotropic and $\mathcal{G}_i^{ss} = \frac{1}{2Vk} \left(t_i^{\mathcal{G}^{ss}}\right)^2$, where $t_i^{\mathcal{G}^{ss}} = k \sum_j e_j^{\mathcal{G}^{ss}} S_{i,j}$ is the tension in a bond for a shear deformation. With these assumptions, $t_i^{\mathcal{G}^{ss}}$ can be regarded as a sum of independent random variables with zero mean. Since $S_{i,j}^2$ decays as function of distance[26, 27], $t_i^{\mathcal{G}^{ss}}$ is dominated by the bonds that lie within this correlation length. According to the central limit theorem, bonds with a given value of S_i^2 are Gaussian distributed with zero average and a variance $\left\langle \left(t_i^{\mathcal{G}^{ss}}\right)^2 \right\rangle \propto \left\langle \mathcal{G}^{ss} \left(S_i^2\right) \right\rangle \propto S_i^2$, as shown in Fig 1. To place all bonds on the same scale we divide the tension by $\sqrt{S_i^2}$, such that the overall distribution of $t_i^{\mathcal{G}^{ss}}/\sqrt{S_i^2}$ is Gaussian. The distribution of $\Delta \mathcal{G}^{ss} \propto (t_i^{\mathcal{G}^{ss}})^2/S_i^2$ can be then obtained through a change of variables. This argument is valid for all the independent shear moduli, $\mathcal{G}$. This leads to

$$P\left(\frac{\Delta \mathcal{G}_i}{\langle \Delta \mathcal{G}_i \rangle} = y\right) = \frac{1}{\sqrt{2\pi}} y^{-\frac{1}{2}} e^{-\frac{y}{2}}, \qquad (11)$$

consistent with our numerical results in Fig. 2(c).

Why does pruning bonds in many cases drive ΔB_i towards the universal distribution of Eq. 11? In contrast to a shear deformation, the affine extension in compression $e_i^B = \epsilon |\delta r_i|$ is non-negative. As a result, we cannot assume that t_i^B averages to zero. Furthermore, at long distances $\langle [S_i]_j \rangle \propto \frac{1}{N}$; this is a consequence of the special state of self stress that arises just above the onset of jamming and accounts for the nonzero value of the bulk modulus there. We suspect that pruning bonds destroys this state of self stress so that once again, t_i^B can be considered the sum of uncorrelated random variables with zero average. In the same manner, if $\langle B_i \rangle \propto S_i^2$, then $t_i^B/\sqrt{S_i^2}$ have a zero average and are Gaussian distributed. This leads directly to the universal distribution for $P\left(\Delta B_i\right)$.

We also show the distribution $P(S_i^2)$ in the solid curves of Fig. 2(d). At low S_i^2: $P(S_i^2) \sim \left(S_i^2\right)^{-\theta_s = -0.42 \pm 0.02}$. This power law is robust to changes of ΔZ. To understand this, we argue that $P(S_i^2)$ is directly related to the distribution of interparticle forces, $P(F)$, in the original jammed system from which the spring network was derived. Suppose the system has one bond above the minimum needed for isostaticity, where there is only one state of self stress. In this limit, force balance specifies a unique set of forces on the bonds so that the state of self stress is uniquely defined: $s_i \propto F_i$ [28] and $S_i^2 = s_i^2$. The distribution of forces, $P(F)$, has a power-law tail at small forces in this limit, such that $P(F) \sim F^\theta$, where the mean-field value of $\theta = 0.17462$ [29] is consistent with numerical results in dimensions down to $d = 2$ [8, 30]. Using a transformation of variables between F_i and S_i^2 to obtain $P(S_i^2)$ from $P(F_i)$, we find $P\left(S_i^2\right) \propto \left(S_i^2\right)^{(\theta-1)/2}$. Thus, we predict $\theta_s = (1 - \theta)/2 = 0.41269...$, in good

agreement with the solid curves in Fig. 2(d). Note that the result remains robust even as ΔZ increases well above the minimum needed for rigidity. In Appendix C we trace this power law to particles with the $d+1$ contacts – the minimum number of contacts needed for local stability.

VII. DISCUSSION

At large length scales, periodic and disordered networks are both governed by elastic theory and their macroscopic mechanical response is captured by global elastic constants. At the bond level, however, periodic and disordered networks exhibit different behavior. For periodic networks, in which a unit cell of a few nodes is repeated throughout, each bond i has a similar local modulus, S_i^2. In addition each bond plays a similar role in resisting global deformations, so that M_i is similar for different global moduli M, and has a similar effect on those moduli if it is removed. Thus ΔM_i is similar for different M. Disordered networks are completely different –the distributions of S_i^2, M_i and ΔM_i are broad and stretch continuously down to zero. Variations in single-bond responses are important not only for tuning global moduli, but also for controlling the response of the system to stresses that are high enough to break bonds, and ultimately to fracture the material.

We have shown that theoretical insight can be gained by studying a new local modulus that describes the response of a network to the change of the equilibrium length of bond i. This relates the contribution M_i of bond i to a global modulus M, to the change of the modulus ΔM_i when bond i is removed, and explains why $\mathcal{G}_i$ and B_i have significant correlations while $\Delta \mathcal{G}_i$ and ΔB_i do not. We have further shown that the distribution of ΔM_i is universal (at least after sufficient pruning) with a form that can be understood.

With these results, we can now understand why the ratio of $\mathcal{G}/B$ is so tunable in disordered networks in terms of the local modulus of a bond L_i. Tunability requires independence of bond-level response, which relies on two properties: (1) that the distributions of $\Delta \mathcal{G}_i$ and ΔB_i are broad, continuous and extend continuously to $\Delta \mathcal{G}_i = 0$ and $\Delta B_i = 0$, and (2) that $\Delta \mathcal{G}_i$ and ΔB_i are uncorrelated. The local modulus provides significant understanding of both of these properties.

VIII. APPENDIX

A. Bond removal formula for non-identical spring constants

In the main text, we derived the equation $\Delta M_i = M_i/S_i^2$ relating ΔM_i, the change of the modulus M when bond i is removed, to M_i, the contribution of bond i

to M, and S_i^2, the local modulus, for the special case in which all the bonds in the networks have the same spring constant. Here we show that the same equation holds more generally, for arbitrary spring constants on the bonds.

We follow the framework of Ref. [14], where the energy, is given by :

$$E = \frac{1}{2}e_s^T \left(\left(k^{-1} \right)_{ss} \right)^{-1} e_s \tag{12}$$

where e_s is the projection of the affine bond extensions on to the space of states of self stress (T denotes transpose); $k_{ij} = \delta_{ij}k_i$ is the matrix of the spring constants and the subscript ss the projection on to the space of state of self stress. We begin our analysis by selecting an arbitrary basis of states of self stress s_α and rewrite Eq. 1 in this basis.

$$E = \frac{1}{2} \sum_{\alpha\beta} e_\alpha p_{\alpha\beta}^{-1} e_\beta \tag{13}$$

where $e_\alpha = \sum_i e_i s_{\alpha,i}$. For convenience we introduce $p_{\alpha\beta} = \left(k_{ss}^{-1} \right)_{\alpha\beta} = \sum_{ij} s_{\alpha,i} \left(k_{ss}^{-1} \right)_{ij} s_{\beta,j}$ which, by construction, is projected onto the space of states of self stress.

Varying the spring constant of bond i , modifies only a single component in the spring constant matrix, $k_{ii}'^{-1} = k_{ii}^{-1} + \left(\frac{1}{k_i'} - \frac{1}{k_i} \right)$. The resulting change in p is given by

$$p_{\alpha\beta}' = p_{\alpha\beta} + \left(\frac{1}{k_i'} - \frac{1}{k_i} \right) s_{\alpha,i} s_{\beta,i} \tag{14}$$

To compute the resulting energy using Eq. 1 we require $(p')^{-1}$ which can conveniently be computed using the Sherman–Morrison formula[31],

$$p_{\alpha\beta}'^{-1} = p_{\alpha\beta}^{-1} - \frac{\left(\frac{1}{k_i'} - \frac{1}{k_i} \right) \sum_{\gamma\delta} p_{\alpha\gamma}^{-1} s_{\gamma,i} s_{\delta,i} p_{\delta\beta}^{-1}}{1 + \left(\frac{1}{k_i'} - \frac{1}{k_i} \right) \sum_{\gamma\delta} s_{\gamma,i} p_{\gamma\delta}^{-1} s_{\delta,i}}. \tag{15}$$

Removing a bond corresponds to taking the limit $k_i' \to 0$, which leads to

$$p_{\alpha\beta}'^{-1} = p_{\alpha\beta}^{-1} - \frac{\sum_{\gamma\delta} p_{\alpha\gamma}^{-1} s_{\gamma,i} s_{\delta,i} p_{\delta\beta}^{-1}}{\sum_{\gamma\delta} s_{\gamma,i} p_{\gamma\delta}^{-1} s_{\delta,i}}. \tag{16}$$

Thus the change in energy is give by,

$$\Delta E = \frac{1}{2} \frac{\sum_{\alpha\beta\gamma\delta} e_\alpha p_{\alpha\gamma}^{-1} s_{\gamma,i} s_{\delta,i} p_{\delta\beta}^{-1} e_\beta}{\sum_{\gamma\delta} s_{\gamma,i} p_{\gamma\delta}^{-1} s_{\delta,i}}, \tag{17}$$

and all that remains is to recast this expression in terms of M_i and S_i^2.

We begin with the denominator and show that it corresponds to a localized deformation. To this end, we select $e_j = e_0 \delta_{ij}$ in Eq. 12 and find that S_i^2, defined as the local modulus per-unit spring constant, is indeed given by the denominator.

$$S_i^2 = \frac{2E}{k_i e_0^2} = \frac{1}{k_i} \sum_{\gamma\delta} s_{\gamma,i} p_{\gamma\delta}^{-1} s_{\delta,i}. \tag{18}$$

We now turn to show that the numerator in Eq. 17 is M_i. Following the derivation of Eq. 1, in Ref. [14] it is straightforward to show that the tension in a bond is given by

$$t = \left(\left(k^{-1} \right)_{ss} \right)^{-1} e_s. \tag{19}$$

In our choice of basis,

$$t_i = \sum_{\alpha\beta} s_{\alpha,i} p_{\alpha\beta}^{-1} e_\beta \tag{20}$$

and therefore the numerator in Eq. 17 is equal to t_i^2. Recalling that the modulus $M = 2E/e_0^2$, we find that

$$\Delta M_i = \frac{M_i}{S_i^2}. \tag{21}$$

B. Two-dimensional data

In this section we test the robustness of the three dimensional results presented in the paper, by comparing them to their two dimensional counterparts. Fig. 3a and 3b shows $\langle B_i \left(S_i^2 \right) \rangle$ and $\langle \mathcal{G}_i \left(S_i^2 \right) \rangle$ for different values of ΔZ. Similarly to the three dimensional case, over a broad range these are proportional of S_i^2 with $\langle \mathcal{G}_i \left(S_i^2 \right) \rangle$ virtually independent of ΔZ, while $\langle B_i \left(S_i^2 \right) \rangle$ has a multiplicative dependence $\Delta Z^{\approx -1.4}$. Three dimensions has a little different dependence on ΔZ, $\langle B_i \left(S_i^2 \right) \rangle \propto \Delta Z^{\approx -1} S_i^2$. A possible source of this variation is that in two dimensions $\langle B_i \left(S_i^2 \right) \rangle$ has a more pronounced plateau at large S_i^2 values.

Fig. 4 considers correlations between B_i and $\mathcal{G}_i$, and the correlations between ΔB_i and $\Delta \mathcal{G}_i$. Fig. 4a shows that distribution of B_i depends on the range $\mathcal{G}_i$ values implying that these are correlated. On the other hand the distribution of ΔB_i, shown in Fig. 4b, appears to be independent of $\Delta \mathcal{G}_i$ suggesting tiny amount of correlations. The behavior in two dimensions appear identical to the behavior in three dimensions. We also find little difference in the distributions of B_i, $\mathcal{G}_i$, ΔB_i and $\Delta \mathcal{G}_i$ between two and three dimensions and in fact, Fig. 2c in main text shows cases where they are identical.

Fig. 5 shows the distribution of S_i^2 as a function of ΔZ. Also here, there is no apparent difference from the three dimensional case and the exponent characterizing

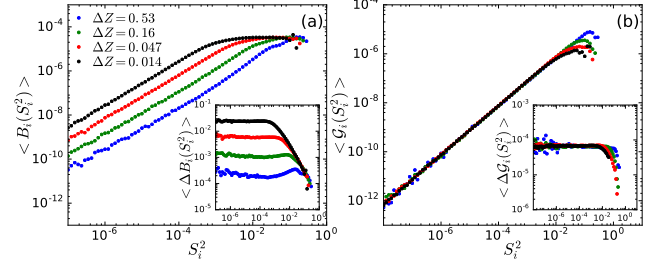the power-law scaling at small S_i^2 agrees with the prediction $P \left(S_i^2 \right) \propto \left(S_i^2 \right)^{-0.41269}$.

Figure 3. a) The conditional average $\langle B_i \left(S_i^2 \right) \rangle$ and b) $\langle \mathcal{G}_i \left(S_i^2 \right) \rangle$ are proportional to S_i^2 over a broad range of S_i^2. In the inset the corresponding $\langle \Delta B_i \left(S_i^2 \right) \rangle$ and $\langle \Delta \mathcal{G}_i \left(S_i^2 \right) \rangle$ are shown. To good approximation these are independent of S_i^2 except at high S_i^2. Data is from 2d systems with $N = 8192$ particles.
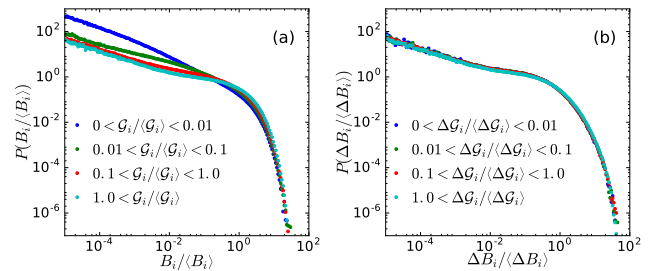

Figure 4. a) $P \left(B_i \right)$ for different ranges of $\mathcal{G}_i$ and b) $P \left(\Delta B_i \right)$ for different range of $\Delta \mathcal{G}_i$ in two dimensions. The collapse indicates almost vanishing correlations. Here $\Delta Z = 0.047$ and the number of particles $N = 8192$.
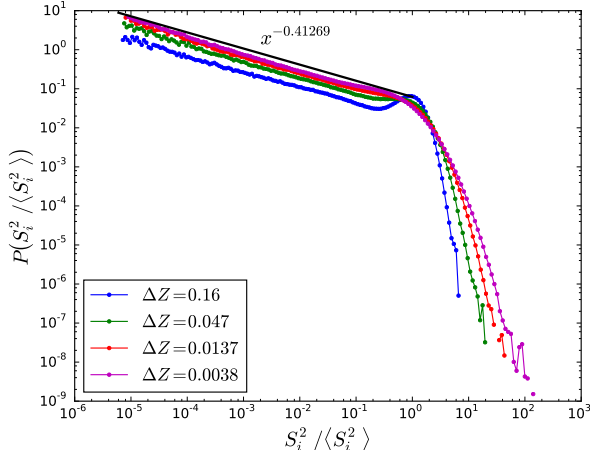
Figure 5. $P\left(S_i^2\right)$ at different values of ΔZ in two dimensions with $N = 8192$ particles. The exponent 0.41269... is the prediction based on the contribution from bucklers[8, 30]. Note that as ΔZ is increased a peak in $P\left(S_i^2\right)$ develops.

C.   Effect of "bucklers" on $P\left(S_i^2\right)$

In this section we show that the scaling of $P\left(S_i^2\right) \propto \left(S_i^2\right)^{-\theta_S \approx -0.42}$ at small S_i^2 results from particular particles with $d + 1$ neighbors called "bucklers". To this end we consider the distribution of S_i^2 when these particles are not included. The scaling argument in the main text is based on the behavior at isostaticity where the distribution of forces, $P\left(F\right) \propto F^\theta$ at small F. As we argued in the main text

$$\theta_s = 1/2 - \theta/2. \tag{22}$$

The exponent θ has two contributions [30] – (1) The mean-field exponent [29, 32] $\theta^{(\infty)} = 0.42311...$ and (2) The exponent due to "buckler" particles $\theta = 0.17462...$, which overshadows the first contribution. Buckler particles are those with $d + 1$ interacting neighbors in d dimensions, for which d forces are nearly balanced across the particle in what is nearly a line in $d = 2$ or a plane in $d = 3$, while the remaining force is very small. In the main text, we showed that Eq. 22 holds if all particles and forces are included. If bucklers are removed, the force distribution scales as $P(F) \sim F^{\theta^{(\infty)}}$ at small F [30]. We would therefore expect the exponent in $P(S_i^2)$ to change when bucklers are removed. Indeed, the prediction of Eq. 22 that $\theta_S^{(\infty)} = 0.28845...$ is in good agreement with our numerical results at the lowest value of ΔZ shown in Fig. 4. Note that once bucklers are removed, however, the exponent θ_S is not robust to changes in ΔZ; Fig. 4 shows that $P\left(S_i^2\right)$ approaches a constant at small S_i^2 as ΔZ increases. Comparing Fig. 5 to Fig. 2d of the main text we deduce that bucklers are the origin of the small

$P\left(S_i^2\right)$ scaling seen in Fig. 2d of the main text, which, interestingly, depends only weakly on ΔZ.

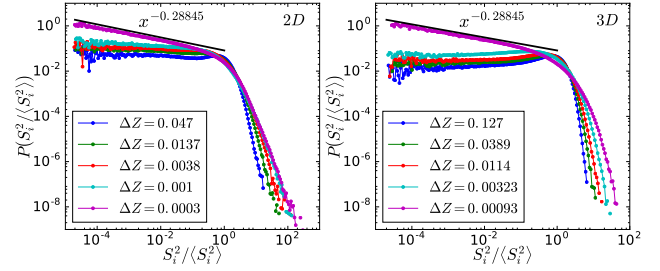Figure 6. $P\left(S_i^2\right)$ in two dimensions (left) and three dimensions (right) when buckler particles are removed. The exponent 0.28845 is the prediction based on the the mean-field scaling of $P\left(F\right)$ at isostaticity . Note that the smallest ΔZ curve is different from the remaining curves with larger ΔZ, suggesting that the exponent is not robust to the increase of ΔZ unlike the buckler contribution.

----

* danielhe2@uchicago.edu

[1] M. Tsamados, A. Tanguy, C. Goldenberg, and J.-L. Barrat, Phys. Rev. E **80**, 026112 (2009).

[2] S. Alexander, Physics Reports **296**, 65 (1998).

[3] F. H. Stillinger, The Journal of Chemical Physics **89**, 6461 (1988), https://doi.org/10.1063/1.455365.

[4] M. L. Manning and A. J. Liu, Phys. Rev. Lett. **107**, 108302 (2011).

[5] D. Bonamy and E. Bouchaud, Physics Reports **498**, 1 (2011).

[6] M. M. Driscoll, B. Gin-ge Chen, T. H. Beuman, S. Ulrich, S. R. Nagel, and V. Vitelli, ArXiv e-prints (2015), arXiv:1501.04227.

[7] C. P. Goodrich, A. J. Liu, and S. R. Nagel, Phys. Rev. Lett. **114**, 225501 (2015).

[8] E. Lerner, G. During, and M. Wyart, Soft Matter **9**, 8252 (2013).

[9] H. Mizuno, S. Mossa, and J.-L. Barrat, Phys. Rev. E **87**, 042306 (2013).

[10] C. Calladine, International Journal of Solids and Structures **14**, 161 (1978).

[11] J. C. Maxwell, Philosophical Magazine Series **27**, 294 (1864).

[12] S. Pellegrino and C. Calladine, International Journal of Solids and Structures **22**, 409 (1986).

[13] S. Pellegrino, International Journal of Solids and Structures **30**, 3025 (1993).

[14] T. C. Lubensky, C. L. Kane, X. Mao, A. Souslov, and K. Sun, Reports on Progress in Physics **78**, 073901 (2015).

[15] M. Wyart, Ann. Phys. Fr. **30**, 1 (2006).

[16] To find $|s_1\rangle$ we assume an arbitrary basis $|s_\alpha*\rangle$ and then $|s_1\rangle = C \sum_\alpha \langle e^M \mid s_\alpha*\rangle |s_\alpha*\rangle$ where C is a normalization constant. This satisfies by definition $\langle e \mid s_\alpha \rangle = 0$ for all $\alpha > 1$.

[17] $S_{i,j}$ is related to the dipole response studied in [26, 27] and decays as a function of distance between bonds with a characteristic length scale that diverges as $\Delta Z \to 0$.

[18] The equality can be verified by noting that $S_{i,j}$ is the i, j component of the projection matrix $\sum_\alpha |s_\alpha\rangle \langle s_\alpha|$ such that $\sum_j S_{i,j} S_{j,k} = S_{i,k}$.

[19] D. J. Durian, Phys. Rev. Lett. **75**, 4780 (1995).

[20] A. J. Liu and S. R. Nagel, Annu. Rev. Condens. Matter Phys. **1**, 347 (2010).

[21] C. P. Goodrich, S. Dagois-Bohy, B. P. Tighe, M. van Hecke, A. J. Liu, and S. R. Nagel, Phys. Rev. E **90**, 022138 (2014).

[22] C. P. Goodrich, A. J. Liu, and S. R. Nagel, Phys. Rev. Lett. **109**, 095704 (2012).

[23] L. E. Silbert, A. J. Liu, and S. R. Nagel, Phys. Rev. E **73**, 041304 (2006).

[24] W. G. Ellenbroek, Z. Zeravcic, W. van Saarloos, and M. van Hecke, EPL **87**, 34004 (2009).

[25] We note that small systems posses finite-size effects; in the extreme limit of $N(Z - Z_{iso}) = 1$ where N is the number of nodes in the network all deformations are necessarily correlated. The correlations quoted above are for systems large enough so that $N(Z - Z_{iso}) >> 1$).

[26] E. Lerner, E. DeGiuli, G. Düring, and M. Wyart, Soft Matter **10**, 5085 (2014).

[27] D. M. Sussman, C. P. Goodrich, and A. J. Liu, Soft Matter (2016), 10.1039/C6SM00094K.

[28] The proportionality constant is fixed by normalization s_i to have unit norm.

[29] P. Charbonneau, J. Kurchan, G. Parisi, P. Urbani, and F. Zamponi, Nature Communications **5**, 3725 (2014).

[30] P. Charbonneau, E. I. Corwin, G. Parisi, and F. Zamponi, Phys. Rev. Lett. **114**, 125504 (2015).

[31] J. Sherman and W. J. Morrison, Ann. Math. Statist. **21**, 124 (1950).

[32] P. Charbonneau, J. Kurchan, G. Parisi, P. Urbani, and F. Zamponi, Journal of Statistical Mechanics: Theory and Experiment **2014**, P10009.